



UNIVERSITY OF LEEDS

This is a repository copy of *Turbidite bed thickness statistics of architectural elements in a deep-marine confined mini-basin setting: Examples from the Grès d'Annot Formation, SE France*.

White Rose Research Online URL for this paper:
<http://eprints.whiterose.ac.uk/130983/>

Version: Accepted Version

Article:

Pantopoulos, G, Kneller, BC, McArthur, AD et al. (3 more authors) (2018) Turbidite bed thickness statistics of architectural elements in a deep-marine confined mini-basin setting: Examples from the Grès d'Annot Formation, SE France. *Marine and Petroleum Geology*, 95. pp. 16-29. ISSN 0264-8172

<https://doi.org/10.1016/j.marpetgeo.2018.04.008>

© 2018 Elsevier Ltd. All rights reserved. This is an author produced version of a paper published in *Marine and Petroleum Geology*. Uploaded in accordance with the publisher's self-archiving policy.

Reuse

Items deposited in White Rose Research Online are protected by copyright, with all rights reserved unless indicated otherwise. They may be downloaded and/or printed for private study, or other acts as permitted by national copyright laws. The publisher or other rights holders may allow further reproduction and re-use of the full text version. This is indicated by the licence information on the White Rose Research Online record for the item.

Takedown

If you consider content in White Rose Research Online to be in breach of UK law, please notify us by emailing eprints@whiterose.ac.uk including the URL of the record and the reason for the withdrawal request.



eprints@whiterose.ac.uk
<https://eprints.whiterose.ac.uk/>

Turbidite bed thickness statistics of architectural elements in a deep-marine confined mini-basin setting: Examples from the Grès d'Annot Formation, SE France.

G. Pantopoulos¹, B.C. Kneller², A.D. McArthur^{1,3}, S. Courivaud¹, A.E. Grings¹, J. Kuchle¹

¹ Instituto de Geociências, Universidade Federal do Rio Grande do Sul (UFRGS), Porto Alegre, RS, 91501-970, Brazil

² Department of Geology & Petroleum Geology, University of Aberdeen, Aberdeen, AB24 3UE, UK

³ School of Earth and Environment, University of Leeds, Leeds, LS2 9JT, UK

Abstract

Statistical analysis of bed thickness was performed for sampled turbidite successions from well-documented architectural elements of the Grès d'Annot Formation to characterise confined deep-water mini-basins of the Tertiary foreland basin of SE France. The purpose was to use advanced statistical processing techniques in order to evaluate whether a discrimination of different architectural elements is feasible through observed statistical signatures of bed thickness. Statistical methods were focused on: i) fitting of widely used non-normal theoretical distribution models using robust non-parametric goodness-of-fit statistical tests, and ii) detecting the possible presence of non-random bed thickness clustering using existing and new clustering estimation methods. Results indicate that the bed thickness data are best characterized by a multi-modal lognormal distribution model which probably reflects a background sedimentological process. Several datasets exhibit power law as well as exponential thick-bedded tails. The data also exhibit non-random clustering of bed thickness. Discrimination of architectural elements in this confined turbidite succession seems to be feasible based

on the characteristics of the observed composite lognormal distributions such as number and variability of the detected components. The estimation of the degree of facies clustering has potential for the discrimination of architectural elements in confined basin settings if used in conjunction with alternative estimation methods (such as periodogram estimation). This methodology may now be applied to other confined turbidite successions, be they outcrops with less certain architecture, or subsurface datasets with borehole imaging.

Keywords: deep-water, bed thickness distribution, facies clustering, power law, lognormal, Grès d'Annot, Eocene.

Introduction

Statistical knowledge regarding the thickness and stratal patterns of deep-marine gravity flow deposits (turbidites) constitutes an important aspect of recent sedimentological research since turbidite deposits can host large hydrocarbon accumulations. Thus, information such as the thickness distribution of turbidite beds in a vertical section can be an important component in the creation of reservoir models and the estimation of reservoir volumes (e.g. Flint & Bryant, 1993; Drinkwater & Pickering, 2001; Sylvester, 2007). Therefore, a detailed statistical characterization and methodology is essential in order to better constrain reservoir modelling parameters for turbidite deposits. Furthermore, the characteristics of turbidite bed thickness distributions (Malinverno, 1997; Carlson and Grotzinger, 2001; Talling, 2001; Mattern, 2002; Sinclair and Cowie, 2003; Clark and Steel, 2006) or the degree of turbidite facies clustering (Chen and Hiscott, 1999) might prove useful in differentiating depositional settings, even when working with data of limited lateral extent, such as wells or isolated outcrops (Sylvester, 2007).

Previous studies have attempted to assess the possibility of characterizing turbidite depositional environments based on observed types of bed thickness statistical distributions (Carlson and Grotzinger, 2001; Talling, 2001; Sylvester, 2007; Prekopová and Janočko, 2009; Pantopoulos et al., 2013), and bed thickness clustering (Chen and Hiscott, 1999; Mukhopadhyay et al., 2003; Felletti, 2004; Felletti and Bersezio, 2010b; Kötelešová, 2012; Pantopoulos et al., 2013).

This study presents the results of statistical analysis of turbidite bed thickness data from well-documented architectural elements in a confined mini-basin setting of the Grès d'Annot Formation, SE France (Fig.1; Hilton, 1994; Amy et al., 2000; Amy et al., 2004; Puigdefàbregas et al., 2004; Amy et al., 2007), focusing on fitting of statistical distributions and quantitative recognition of facies clustering. The main objectives of this study are: a) to determine whether the empirical distribution of turbidite thicknesses of well documented architectural elements can be expressed by a specific theoretical distribution model using advanced statistical goodness-of-fit methods, b) to estimate possible discrimination of architectural elements based on the best fitting distribution model, where these elements have been previously defined, and c) to assess the usefulness of facies clustering techniques by combined testing of new and previously proposed methodologies on sampled bed thickness data.

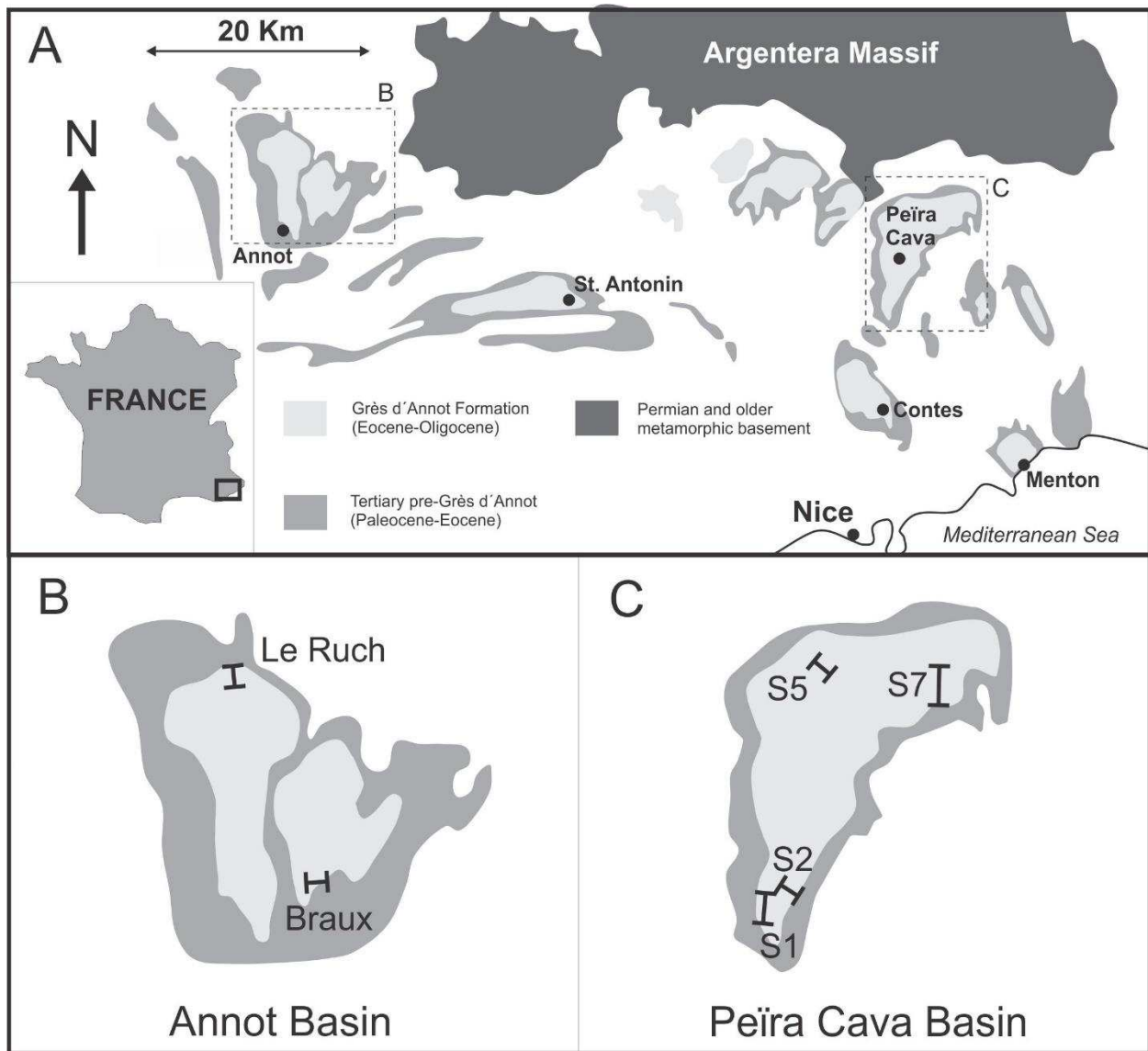


Figure 1: A) Simplified geological map of southeastern France highlighting the outcropping remnants of the Grès d'Annot Formation. The locations of the studied outcrops at B) Annot and C) Peira Cava sub-basins. Modified from Amy (2000).

Geological Setting

The Grès d'Annot Formation was deposited during the late Eocene to early Oligocene (du Fornel et al., 2004) in the Tertiary Alpine foreland basin, and is a characteristic example of a confined sand-rich turbidite system, offering good quality exposures over a large area of SE France (Fig. 1; Joseph & Lomas

2004). It occurs as a number of isolated remnants of what was a once a continuous basin (Apps et al., 2004).

The Cenozoic sequence rests with erosional unconformity on a Mesozoic basement. The oldest Tertiary deposits are conglomerates and sandstones, with gravel bars that are rarely capped by palaeosol and coally horizons (Argens Conglomerates). A regionally extensive shallow marine bioclastic limestone unit (Calcaires Nummulitiques Formation) consisting of a variety of bioclastic shallow marine environments commonly characterized by the presence of giant nummulite foraminifera, overlies the previous deposits (Apps et al., 2004). The Marnes Bleues Formation succeeds the Calcaires Nummulitiques and represents a deep-water, marl-dominated succession deposited during a phase of rapid subsidence and low sediment supply (Stanbrook & Clark, 2004).

The final phase of basin fill is dominated by deep-marine clastics derived from the Pyreneo-Provençal orogen to the south, and mass wasting deposits of the advancing Alpine Orogeny (Sinclair, 1997). Deep-marine deposits consist of turbidites of the Priabonian to Rupelian Grès d'Annot Formation which constitutes a 500-1500 m thick, sand-rich succession of turbidites and associated mudstones (Ravenne et al., 1987). At the time of turbidite deposition ongoing regional thrust tectonics created a province of piggy-back basins in which structural highs bounded confined sub-basins (Apps et al. 2004) with a general sediment transport northwards from the Corsica-Sardinia massif (Stanley & Mutti 1978). As turbidite deposition progressed the basin floor topography was gradually buried as the turbidite fill onlapped and eventually filled the basin fill (Sinclair, 2000), although the thrust system continued to be active during turbidite deposition Apps (1987). The remaining accommodation space was filled by the overlying Schists à Blocs Formation (Apps et al. 2004) ending turbidite deposition in the late Rupelian (du Fornel et al., 2004).

The northern basin remnants of the formation are consisting of channelised, relatively “proximal”, to non-channelised, relatively “distal” sand-rich systems, with rare, basin-wide, debris-flow conglomerates (Elliott et al. 1985; Ravenne et al. 1987; Ghibaudo 1995; Hilton & Pickering 1995; Sinclair 1994). The outcrops north-northwest of Nice (Fig. 1) at Contes and Peïra Cava, comprise the southeastern part of the formation and probably form a part of an older, deeper-water system, though apparently more ponded (Amy et al., 2007). The Annot sub-basin (Fig. 1) was separated from those to the NE and bounded to the SW by palaeo-highs, which Elliott et al. (1985) related to ramps in the underlying thrust system.

Sedimentology

Architectural Elements Sampled

The Grès d'Annot Formation has been the subject of numerous detailed studies in the past (Bouma, 1962; Stanley et al., 1978; Amy et al., 2000; McCaffrey and Kneller, 2001; Kneller and McCaffrey, 2003; Joseph & Lomas, 2004; Amy et al., 2007; McArthur et al., 2016; Tinterri et al., 2016; Cunha et al., 2017)), which have produced an advanced stratigraphic and architectural understanding of the depositional system. A range of architectural elements have been recognised within the deposits in Annot and Peïra Cava sub-basins (Fig. 1) based on field sedimentary logging of excellent outcrop exposures and previous work (Amy et al., 2007; McArthur et al., 2016). These elements reflect a lateral transition from basin margin (onlap) sediments, to proximal sedimentary facies (channel-lobe transition and confined sheet and heterolithic deposits), evolving to medial and distal confined sheet and heterolithics respectively at the more distal parts of the studied sub-basins (Fig. 2).

Peïra Cava basin

The turbidite deposits of this studied mini-basin succession exhibit characteristic variations both in the south to north general palaeocurrent direction, as well as from the bottom to the top of their stratigraphy (Figs. 2, 3). The latter vertical facies variation is thought to represent a “back-stepping” of the depositional system, which onlaps the proximal basin margin to the south (Amy et al., 2007). Detailed stratigraphic analysis from previous studies (Amy, 2000; Amy et al., 2007; McArthur et al., 2016) led to the recognition of certain architectural elements, which are briefly described below.

Lower interval of southern basin area (proximal architectural elements)

This lower interval of the succession in the southern areas of the Peira Cava basin, is generally dominated by proximal turbidite facies mainly characterized by thick-bedded sandstones (Fig. 2A)(Amy et al., 2007; Cunha et al., 2017). Thick-bedded packages of coarse-grained sandstone, frequently characterized by amalgamation, generally dominate the succession, exhibiting complex vertical alternations of sedimentary structures and bedding patterns.

Thick beds (which in some cases exceed 5 m in thickness) of poorly sorted, very coarse- to fine-grained sandstones, which exhibit grain size breaks can be observed. Bed bases are typically sharp and flat with sole marks occasionally present. A range of sedimentary structures such as massive, structureless sandstones grading upwards to planar, cross stratification and ripple lamination can be observed. Bed loading as well as pipes and flame structures are also present. Matrix-supported conglomerate, rich in mudstone clasts can be also seen at the bases of characteristic thick beds, which exhibit tabular, laterally continuous geometries. These laterally continuous, thick, tabular, occasionally amalgamated beds were interpreted as confined sheet deposits. Their tabularity is probably the result of the lack of accommodation space characterizing the totally confined flows within the basin which deposit thick, laterally continuous beds with thick mudstone caps as well (Amy et al., 2007; McArthur et al., 2016). The characteristic tabularity of these beds allows their use as marker beds in correlations

across the mini-basin (Amy et al., 2007). Thin-bedded (heterolithic) turbidite packages are also present but not so frequent. Heterolithic packages usually comprise thin-bedded sandstones, siltstones and mudstones. Thin (usually less than 10 cm), medium- to very fine-grained sandstones grade into siltstone with mudstone caps. Sandstone beds are generally characterized by sharp, flat bases and they occasionally show planar and ripple lamination, which may be multi-directional. Alternation between planar and asymmetric ripple lamination characterized by sharp grain size breaks can be also observed. Sole structures are rarely observed. Mudstone intervals are generally thick, show internal variation and contain abundant marine microfossils (McArthur et al., 2016). Thick mudstone caps were formed due to almost complete confinement of the flows within the basin with minimum overspill. Multi-directional asymmetric ripples are interpreted to be the result of flow reflection against basin margins documented by the abundance of complex rippled beds along the basin's margin, and the scattered palaeocurrents observed in the ripples (Kneller and McCaffrey, 1999; Tinterri et al., 2016). Like thick, basin-wide sheet beds, these heterolithic packages can also be traced across the basin, are more abundant in the northern more distal sections and are interpreted as confined heterolithic deposits.

The sedimentary architecture of this lower, southern part of the succession, suggests extensive erosion and bypass by turbidity flows, but also deposition of a large proportion of their coarser-grained sediment load. These deposits have also been interpreted by previous authors as indicating a zone of extensive scour-and-fill (Hilton, 1994; McCaffrey and Kneller, 2001; Lee et al., 2004). Proximal architectural elements occur only close to the southern margin of the basin and are thought to characterize a zone directly downstream of the inbound margin (Amy et al., 2007). For the purpose of this study, the sampled section from this lower part of the Peira Cava basin was classified as a unified proximal architectural element composed of both proximal confined sheets and heterolithics sampled throughout the succession logged (Figs. 2A, 3).

Upper intervals of southern basin area (medial architectural elements)

The equivalent downstream part of the succession in the upper part of the studied southern sections is dominated by a mixture of architectural elements (based on the architectural element classification of Amy et al., 2007), including thick-bedded packages; continuous megabeds and medium-bedded packages. Based on the architectural element classification of the present study, logged thick- and medium-bedded packages of this part of the succession were classified as medial confined sheets and heterolithics (Figs. 2B, 3). Overall, average sandstone bed thicknesses are generally thinner and the proportion of sandstone is lower in this part of the succession, compared with the lower southern outcrop sections. The studied upper part of the succession in the southern sections is considered to comprise more distal deposits relative to those of the lower part of the southern basin area. These deposits are interpreted as representing the proximal part of a basin-plain environment (Amy et al., 2007).

Northern basin area (distal architectural elements).

The studied parts of the northern sections typically contain finer-grained sandstones capped by relatively thick mudstones (Figs 2C, 2D). These sections are characterized by thinner-bedded deposits in relation with the southern part of the basin. According to Amy et al. (2007), the northern sections are characterized by mixed-bedded packages, with a lesser proportion of thick-bedded sandstones, thin-bedded intervals and continuous megabeds. Based on the architectural element classification of the present study, logged bed packages of this part of the succession were classified as distal confined

sheets and heterolithics (Figs. 2C, 2D, 3). The depositional environment of the northern studied outcrop sections was characterized as sheet-like turbidites of a relatively distal basin-plain setting (Amy et al., 2007; Cunha et al., 2017). Characteristic upward changes in facies in the northern sections similar to that seen in the southern sections is not observed (Fig. 3).

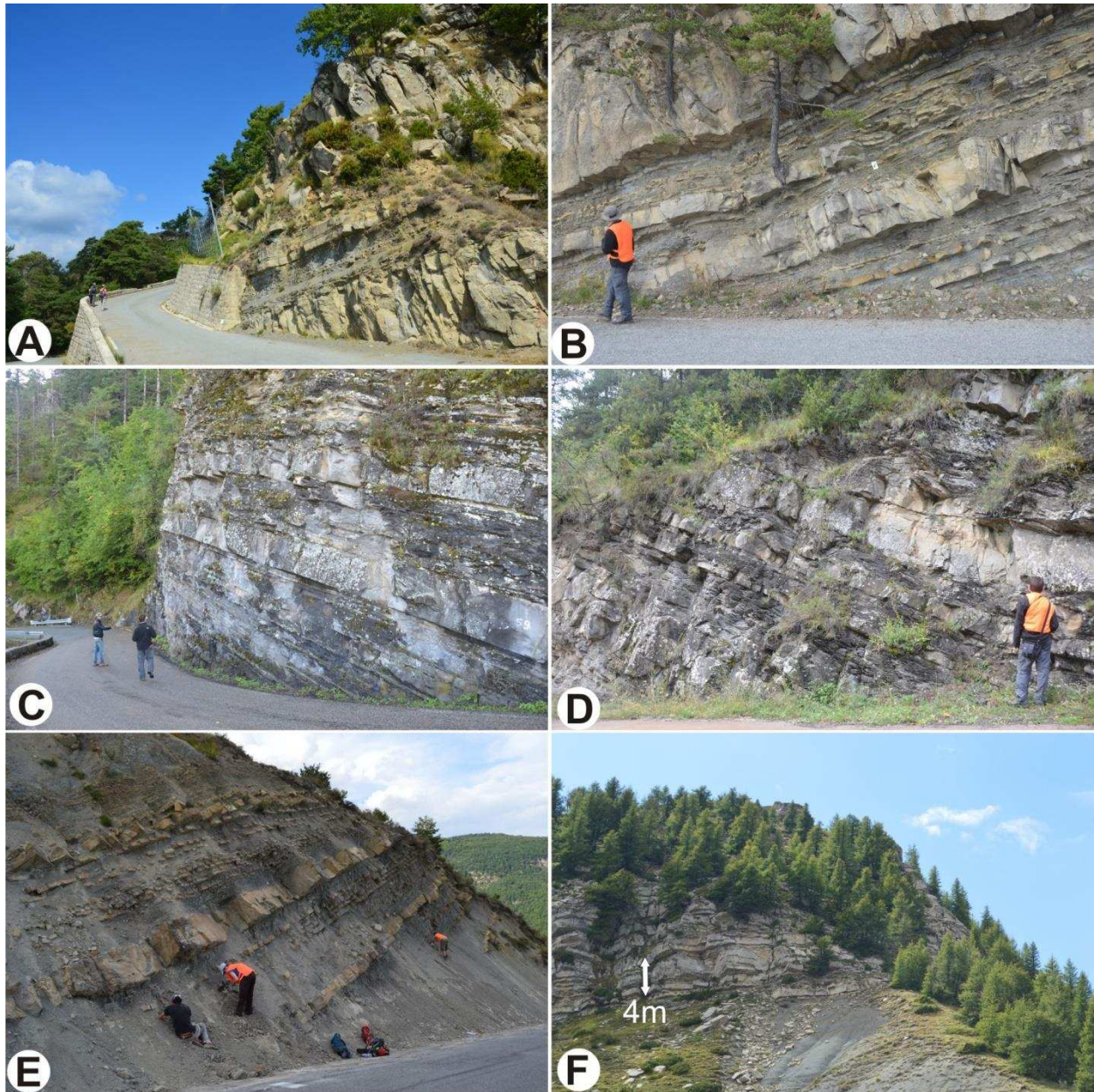


Figure 2: Aspects of logged architectural elements for bed thickness statistical analysis from the Peira Cava and Annot basins of the Grès d'Annot Formation: A) Proximal to medial thick- to medium-bedded confined sheets and heterolithics, Section S1 (Peira Cava basin) B) Medial confined sheets and heterolithics, upper part of Section S2 (Peira Cava basin), C) Distal medium- to thin-bedded confined sheets and heterolithics, Section S5 (Peira Cava basin), D) Distal confined sheets and

heterolithics, Section S7 (Peira Cava basin), E) Basin margin onlap facies, Braux road, (Annot Basin), F) Basin margin onlap, Le Ruch, (Annot Basin).

Annot Basin

Braux and Le Ruch sections (onlap architectural element)

Two additional outcrops were studied in the Annot basin at Braux and Le Ruch areas (Fig. 1). These exposures are characterized by thin- (<10 cm) to medium-bedded (<30 cm), very fine- to medium-grained, well-sorted, laminated or cross-laminated sands grading to mudstones (e.g. Fig. 2E). Repeated truncated laminations and breaks in grain-size are also often observed along with lateral bed pinch-outs. Shearing and slumping is also commonly observed. Packages observed to thin rapidly towards basin margins, overlying and truncating against the Marnes Bleues Formation. Based on the architectural element classification of this study, these deposits were classified as basin margin onlaps. Laterally thinning and truncating thin-beds, with highly variable palaeocurrent orientations are interpreted as low density turbidity current deposits, onlapping and draping over older, tilted slope deposits. These features have previously been interpreted as the result of flows onlapping and reflecting against a major basin margin slope surface (Kneller and McCaffrey, 1999; McCaffrey and Kneller, 2001; Puigdefabregas et al., 2004).

Logged Intervals

Five long stratigraphic intervals were re-logged in detail in four good quality exposures (Sections S1, S2, S5, S7 of Amy et al., 2007) in the Peira Cava mini-basin, representing different architectural elements (Figs. 1, 3): Lower part of Section S2 (proximal sheets and heterolithics element), upper part of Section S1 (proximal to medial sheets and heterolithics element), medial to upper part of Section S2 (medial sheets and heterolithics element), upper part of Section S5 and the lower part of Section S7 (distal sheets and heterolithics element). In addition, two additional logged intervals from characteristic

basin margin onlap elements from the Braux and Le Ruch areas of the Annot basin were logged for statistical analysis of bed thickness.

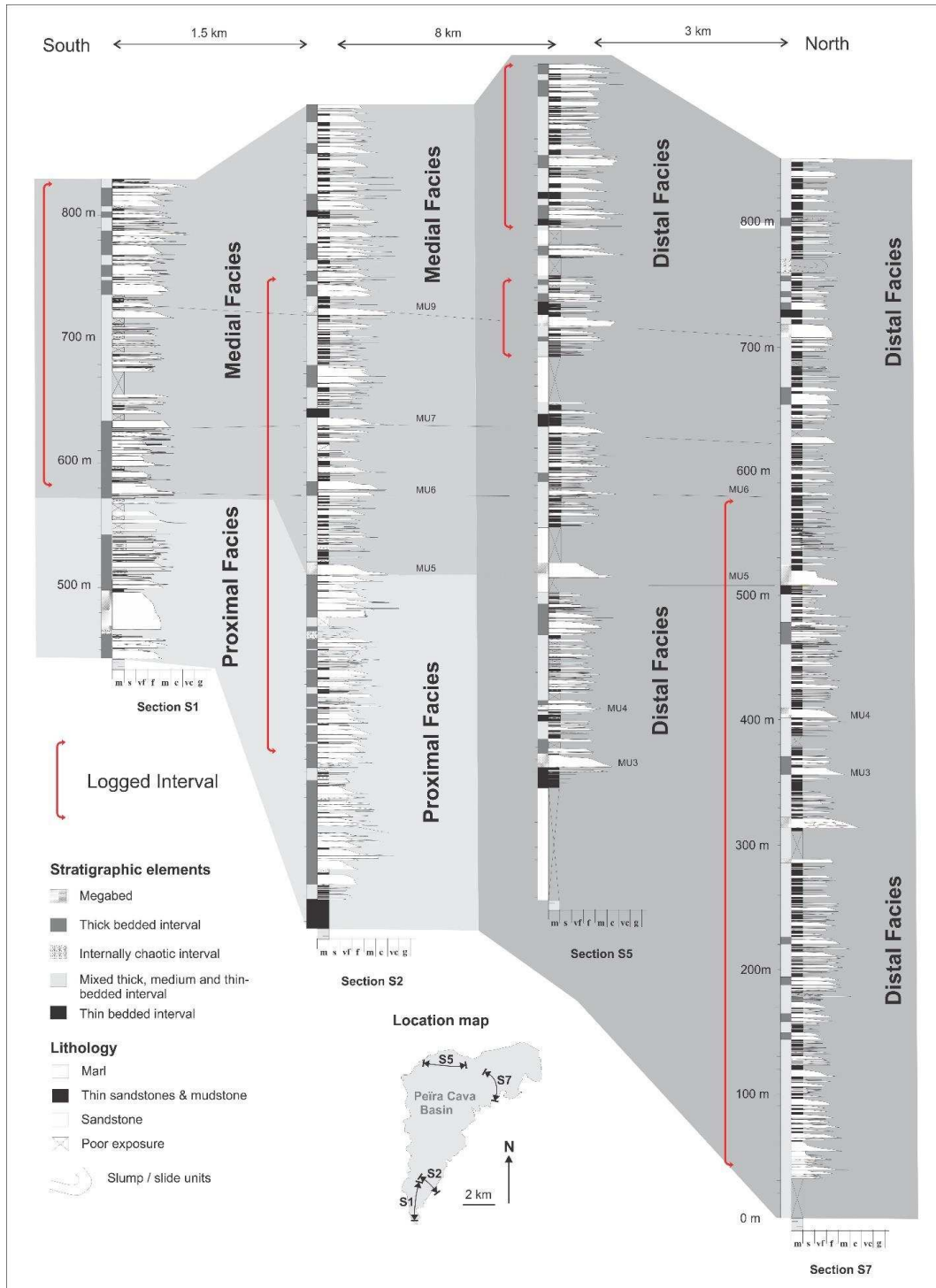


Figure 3: Simplified stratigraphic panel showing studied sections and logged stratigraphic intervals for bed thickness statistical analysis, between outcrop sections of the Peira Cava mini-basin (modified from Amy et al., 2007).

Bed thickness field measurements

For the purpose of this study, the bed unit that was measured represents both the coarse division thickness (sandstone and siltstone) of a turbidite bed (Lowe divisions S_{1-3} and Bouma divisions T_{a-d}) (Bouma, 1962; Lowe, 1982) and also the event thickness which includes the thickness of the capping mud layer. Thickness of capping mudstone layers (Bouma division T_e) in each bed was also taken into account in order to compare the goodness of fit to theoretical statistical models not only of lithologic but also of sedimentation thicknesses as well. The latter approach makes it possible to study how bed thickness relates to bed volume and depositional processes. Discrimination of turbidite from hemipelagic mud was difficult in the field, thus when distinction was possible the thickness of the overlying turbidite mudstone was recorded, otherwise the thickness of the whole capping mud layer was used for statistical analysis. Certain amounts of pale grey, marly and bioturbated (probably oxic) hemipelagites can be observed in the proximal part of the basin. Dark, laminated (probably anoxic) hemipelagic deposits are characterizing the more distal parts of the studied confined succession and their possible effects on event bed thickness distributions is discussed below. A minimum cut-off thickness of 1 cm was established due to measuring difficulties below that thickness. In the case of rippled beds, an average thickness was taken after several measurements. In coarser-grained and thicker-bedded parts of the successions, where amalgamation was frequent, boundaries of individual event sandstone beds were carefully identified by detecting subtle surfaces across which well-defined coarsening occurs. Breaking down amalgamated sections into individual event beds (Sinclair and Cowie, 2003; Sylvester, 2007) has the advantage of making it possible to study how bed thickness relates to depositional processes, whereas the thicknesses of amalgamated units convolve the effects of depositional process and facies clustering (Sylvester, 2007). A minimum number of 100 beds was

measured per section in order for the results to be statistically valid. An exception to the latter rule was applied only for the Braux onlap section of Annot basin, in order to investigate the bed thickness statistical behaviour of a characteristic onlap section where the collection of at least 100 beds was not possible due to outcrop limitations.

Bed Thickness Data

Descriptive statistics of bed thickness data from the seven sections studied (for both coarse division and event thicknesses) are shown in Tables 1 and 2. The total number of beds per section ranges between 180 and 1160 for coarse division (combined sandstone and siltstone thickness) measurements and between 76 and 1158 for turbidite event thickness measurements.

The measured bed thicknesses range from 1 to 1400 cm for coarse divisions and from 3 to 1610 cm for event thicknesses. Means of coarse division thickness for the various sections range from 6.5 to 68.4 cm, while means for event thicknesses range from 13.3 to 74.2 cm. Standard deviation ranges between 10.4 and 135.6 cm for coarse divisions, and 11.5 to 136.9 cm for event thicknesses. Observed high skewness and kurtosis values for both the coarse division and event thicknesses clearly indicate that bed thickness data from all sections are not following a normal (Gaussian) distribution (Tables 1 & 2).

Table 1: Descriptive statistics of turbidite coarse division bed thickness datasets from studied sections of the Grès d' Annot Formation, SE France.

Section	Number of Beds	Min (cm)	Max (cm)	Mean (cm)	Median (cm)	Standard Deviation	Skewness	Kurtosis
<i>Peira Cava</i>								
<i>Basin</i>								
S2 Lower	180	1	700	68.4	9.5	135.6	2.6	6.7
S1 Upper	162	1	840	60.3	10.5	121.8	3.4	14.6
S2 Upper	669	1	860	24.2	4.0	74.9	6.3	49.7

S5	496	1	830	26.6	6.0	74.7	5.8	43.0
S7	1160	1	1400	25.7	5.0	73.1	8.6	121.9
<i>Annot Basin</i>								
Braux	75	1	75	6.5	4.0	10.4	4.4	24.1
Le Ruch	103	1	193	20.9	7.0	39.0	3.1	9.6

Table 2: Descriptive statistics of turbidite event bed thickness datasets from studied sections of the Grès d' Annot Formation, SE France.

Section	Number of Beds	Min (cm)	Max (cm)	Mean (cm)	Median (cm)	Standard Deviation	Skewness	Kurtosis
<i>Peira Cava Basin</i>								
S2 Lower	179	2	702	74.2	15.0	136.9	2.7	7.0
S1 Upper	161	2	850	68.4	20.0	124.8	3.4	14.2
S2 Upper	670	2	890	29.8	9.0	79.5	6.2	48.8
S5	495	2	960	33.2	10.0	81.2	6.1	49.3
S7	1158	2	1610	38.0	11.0	90.7	7.5	92.9
<i>Annot Basin</i>								
Braux	76	3	87	13.3	11.0	11.5	3.8	20.2
Le Ruch	102	2	171	13.9	7.0	20.8	4.8	30.4

Statistical methods

Bed thickness statistical analysis was performed using R software (R Core Team, 2018) and included statistical distribution fitting and bed/facies clustering analysis. Statistical techniques utilized were Maximum Likelihood Estimation (MLE), Expectation-Maximization (EM), Monte Carlo simulation and long range dependence analysis.

Fitting of the lognormal, exponential and power law distributions to bed thickness datasets using MLE techniques and the Kolmogorov-Smirnov (KS) test (Clauset et al., 2009) was implemented using the *powerLaw* R package (Gillespie, 2015). The fitting of a multimodal lognormal distribution to these datasets utilizing EM and Bayesian techniques was investigated using the *mclust* R package (Fraley and Raftery, 2002; Fraley et al., 2012). Facies clustering analysis based on Hurst statistics (Chen and Hiscott, 1999) was implemented based on R code originally proposed by Kötelešová (2012). Alternative

estimation of Hurst statistics based on periodogram estimation techniques (Geweke and Porter-Hudak, 1983) was also implemented using the *fArma* R package (Wuertz, 2015).

Detailed descriptions of these statistical techniques and R packages as well as a brief introduction to observed statistical models of turbidite bed thicknesses can be also found in Chen and Hiscott (1999), Sylvester (2007), Pantopoulos et al. (2013), Palozzi et al. (2018) and references therein..

Results

Power law, lognormal and exponential distributions fitting

Power law, exponential and lognormal distribution fits were tested both for coarse division and sedimentation event bed thicknesses.

Power law distribution goodness-of-fit KS test

Coarse division thicknesses seem to be better characterized by this kind of distribution (in 4 out of 7 cases the power law cannot be rejected) than are event thicknesses, where in 4 out of 7 cases the power law was rejected (KS test p-values < 0.10, Tables 3, 4). However the power law seems to hold only above a certain thickness threshold, which seems to be lower for the onlap sections. In the cases that the power law cannot be rejected by the KS test, it holds for a range of thicker beds that varies from 2.3 to 69.9% of the whole bed population for coarse division thicknesses and from 15.6 to 31.5% for event thicknesses. Larger percentages are generally observed for the onlap sections both for coarse division and event bed thicknesses.

Table 3: Results of the Kolmogorov-Smirnov (KS) goodness-of-fit test for the power law distribution based on Clauset et al. (2009) for coarse turbidite division thicknesses from studied sections.

Section	Power Law Exponent	Threshold (cm)	% of Beds Above Threshold	KS Test Bootstrap p-value (a=0.10)
<i><u>Peira Cava Basin</u></i>				
S2 Lower	-	-	-	0.00
S1 Upper	2.84	170	12.1	0.54
S2 Upper	-	-	-	0.00
S5	-	-	-	0.02
S7	3.80	240	2.3	0.97
<i><u>Annot Basin</u></i>				
Braux	2.51	7	24.3	0.38
Le Ruch	1.92	5	69.9	0.10

Table 4: Results of the Kolmogorov-Smirnov (KS) goodness-of-fit test for the power law distribution based on Clauset et al. (2009) for turbidite event thicknesses from studied sections.

Section	Power Law Exponent	Threshold (cm)	% of Beds Above Threshold	KS Test Bootstrap p-value (a=0.10)
<i><u>Peira Cava Basin</u></i>				
S2 Lower	-	-	-	0.03
S1 Upper	-	-	-	0.00
S2 Upper	-	-	-	0.00
S5	1.93	17	31.5	0.32
S7	-	-	-	0.00
<i><u>Annot Basin</u></i>				
Braux	3.74	16	27.6	0.81
Le Ruch	3.08	25	15.6	0.88

Lognormal distribution goodness-of-fit KS test

Generally event bed thicknesses are better characterized by this kind of distribution than are the coarse division thicknesses (Tables 5, 6). Only bed thickness measurements from the proximal to the base of slope lower part of Section S2 of the Peira Cava basin seem not to be characterized by a

lognormal distribution both for the coarse division and event bed thicknesses. The observed lognormal fits seem to hold only above a certain thickness threshold which represents from 8.7 to 28.1% of the whole bed population for coarse division thicknesses and from 3.6 to 69.7% for event thicknesses respectively. Larger percentages are again observed for the studied onlap sections both for coarse division and event bed thicknesses.

Table 5: Results of the Kolmogorov-Smirnov (KS) goodness-of-fit test based on Clauset et al. (2009) for the lognormal distribution for coarse turbidite division thicknesses from studied sections.

Section	Mean (Log cm)	Standard Deviation (Log cm)	Threshold (cm)	% of Beds Above Threshold	KS Test Bootstrap p-value ($\alpha=0.10$)
<i>Peira Cava</i>					
<i>Basin</i>					
S2 Lower	-	-	-	-	0.01
S1 Upper	5.27	0.67	88	17.9	0.94
S2 Upper	4.50	0.99	36	11.0	0.86
S5	4.53	1.01	36	11.2	0.30
S7	4.51	0.85	80	8.7	0.96
<i>Annot Basin</i>					
Braux	2.56	0.88	10	13.5	0.86
Le Ruch	2.89	1.30	13	28.1	0.51

Table 6: Results of the Kolmogorov-Smirnov (KS) goodness-of-fit test based on Clauset et al. (2009) for the lognormal distribution for turbidite event thicknesses from studied sections of the Grès d' Annot Formation, SE France.

Section	Mean (Log cm)	Standard Deviation (Log cm)	Threshold (cm)	% of Beds Above Threshold	KS Test Bootstrap p-value ($\alpha=0.10$)
<i>Peira Cava</i>					
<i>Basin</i>					
S2 Lower	-	-	-	-	0.05
S1 Upper	5.36	0.63	96	18.0	0.64
S2 Upper	4.69	0.91	51	10.2	0.65
S5	1.14	2.02	23	24.0	0.85
S7	4.90	0.80	227	3.6	0.97
<i>Annot Basin</i>					
Braux	2.35	0.66	8	69.7	0.89
Le Ruch	0.58	1.41	17	16.6	0.99

Exponential distribution goodness-of-fit KS test

Coarse division bed thicknesses seem to be better characterized by this kind of distribution than are event thicknesses (Tables 7, 8). Only bed thickness measurements from the medial upper part of Section S2 of the Peira Cava basin and also from Le Ruche onlap section of the Annot basin cannot be characterized by an exponential distribution for event bed thicknesses. The observed exponential fits hold only above a certain thickness threshold which represents from 4.0 to 23.3% of the whole bed population for coarse division thicknesses and from 4.8 to 69.7% for event thicknesses respectively.

Table 7: Results of the Kolmogorov-Smirnov (KS) goodness-of-fit test based on Clauset et al. (2009) for the exponential distribution for coarse turbidite division thicknesses from studied sections.

Section	Lambda	Threshold (cm)	% of Beds Above Threshold	KS Test Bootstrap p-value ($\alpha=0.10$)
<i>Peira Cava Basin</i>				
S2 Lower	0.004	60	23.0	0.53
S1 Upper	0.052	86	18.5	0.99
S2 Upper	0.007	39	10.3	0.21
S5	0.083	82	7.2	0.61
S7	0.008	38	12.8	0.21
<i>Annot Basin</i>				
Braux	0.031	26	4.0	0.79
Le Ruch	0.017	17	23.3	0.10

Table 8: Results of the Kolmogorov-Smirnov (KS) goodness-of-fit test based on Clauset et al. (2009) for the exponential distribution for turbidite event thicknesses from studied sections.

Section	Lambda	Threshold (cm)	% of Beds Above Threshold	KS Test Bootstrap p-value ($\alpha=0.10$)
<i>Peira Cava Basin</i>				
S2 Lower	0.004	63	22.9	0.57
S1 Upper	0.005	140	15.5	0.97
S2 Upper	-	-	-	0.06
S5	0.006	90	7.6	0.66
S7	0.005	167	4.8	0.99
<i>Annot Basin</i>				

Braux	0.107	8	69.7	0.75
Le Ruch	-	-	-	0.09

Multimodal lognormal distribution goodness-of-fit

Based on observations and proposals from Talling (2001) and Sylvester (2007), a statistical approach to fit a lognormal distribution with more than one component was implemented using the *mclust* statistical package in R software.

Results of EM algorithm and BIC analysis after log-transformation of the bed thickness datasets for both coarse division and event thicknesses (Fig. 4) indicate the presence of normal (Gaussian) mixtures. The components of the observed mixtures vary from 1 to 3 with most datasets composed of 2 components (Tables 9 &10). Only data from the Braux onlap section are composed of a single Gaussian component, reflecting the presence of a single lognormal thickness distribution for both measurement types. Three-component mixtures were detected in three cases: for coarse division thicknesses of Lower S2 and S7 sections, and for event thicknesses of Upper S2 section from the Peira Cava basin. In the latter cases the variances of the three detected Gaussian components seem to be equal for the case of Lower S2 section and unequal for the other two outcrop cases.

In the remaining studied outcrops, log-transformed thicknesses of both measurement types seem to be well-expressed by a mixture of two Gaussian components: Generally the variances of the two components seem to have a tendency to be equal in the outcrops more proximal to the base of slope and onlap, and unequal in the more medial or distal outcrops, with the exception of coarse division thicknesses of the S5 section (Table 10).

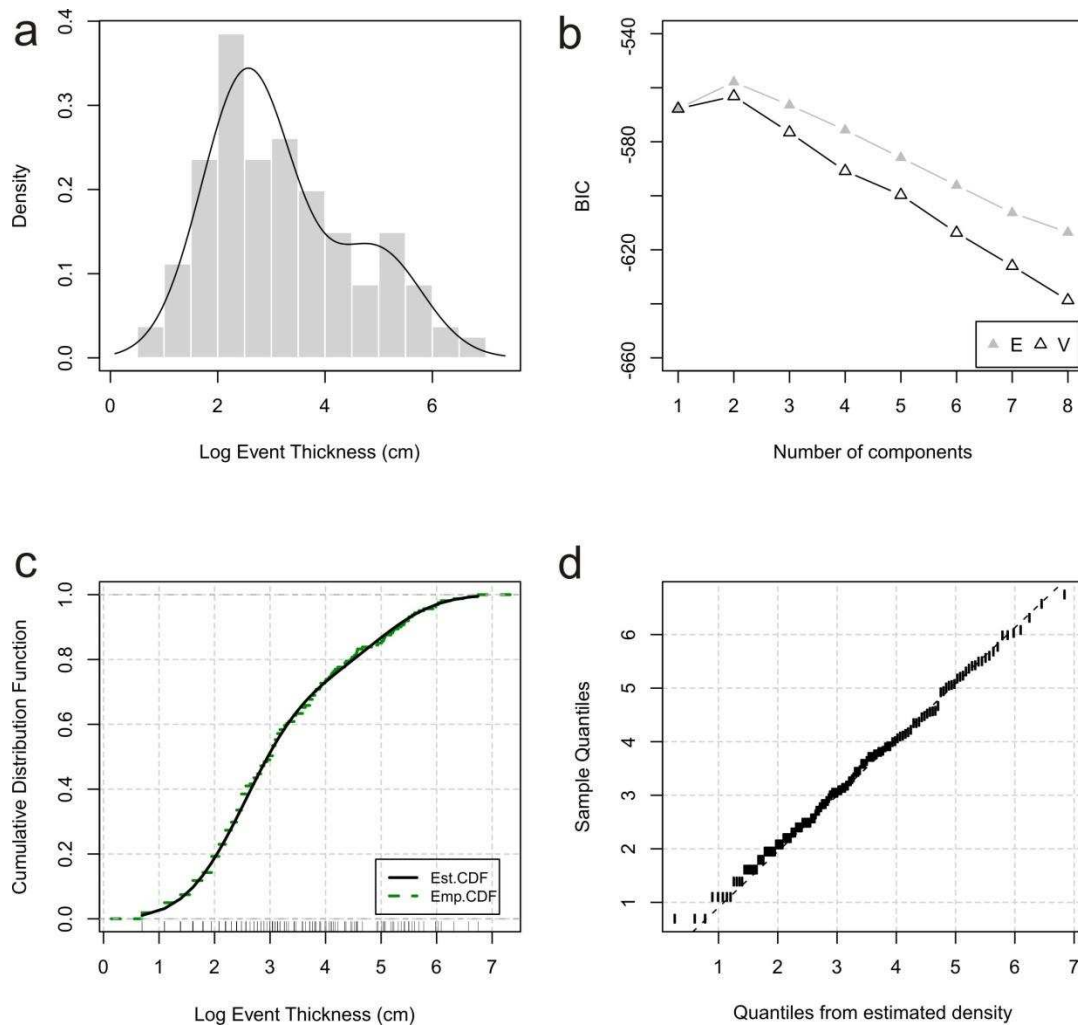


Figure 4: Example of EM/BIC mixture modeling in R software. (a) Multimodal normal mixture density estimate with histogram of log-transformed event thickness data from proximal to medial upper S1 section of the Peira Cava basin, (b) BIC plot for model component selection based on equal (E) or unequal (V) variances. Density estimate diagnostics: (c) plot of estimated CDF and empirical distribution function, (d) Q-Q plot of sample quantiles vs quantiles from density estimation.

Table 9: Results of EM algorithm and BIC analysis for log-transformed turbidite event thicknesses from studied sections.

Section	EM/BIC Detected Gaussian Components (Event Beds)	Relation of Component Variances (Equal- Unequal)	Mixing Probabilities of Detected Components (%)	BIC
S2 Lower (Proximal)	2	Equal	75-25	-623.70
S1 Upper (Proximal/Medial)	2	Equal	73-27	-557.90
S2 Upper (Medial)	3	Unequal (V1<V2<V3)	34-44-22	-1928.63
S5 (Distal)	2	Unequal (V1<V2)	73-27	-1408.94
S7 (Distal)	2	Unequal (V1<V2)	65-35	-3475.17
Braux (Onlap)	1	-	-	-153.21
Le Ruch (Onlap)	2	Equal	84-16	-323.89

Table 10: Results of EM algorithm and BIC analysis for log-transformed turbidite coarse division thicknesses from studied sections.

Section	EM/BIC Detected Gaussian Components (Sand Beds)	Relation of Component Variances (Equal- Unequal)	Mixing Probabilities of Detected Components (%)	BIC
S2 Lower (Proximal)	3	Equal	50-28-22	-698.80
S1 Upper (Proximal/Medial)	2	Equal	64-36	-646.35
S2 Upper (Medial)	2	Unequal (V1<V2)	72-28	-2100.45
S5 (Distal)	2	Equal	89-11	-1561.90
S7 (Distal)	3	Unequal (V1<V2<V3)	32-53-15	-3774.33
Braux (Onlap)	1	-	-	-212.33
Le Ruch (Onlap)	2	Equal	84-16	-333.37

Graphical assessment of the goodness-of-fit to the composite lognormal models using density histograms, CDF and Q-Q plots (Fig. 5) shows a good fit of the detected mixture models to datasets from both measurement types and the best fit among tested distribution models for the whole bed thickness range. More particularly, examination of BIC values (Tables 9, 10) shows higher values for fitted mixture models of event thicknesses in all studied cases, indicating a better fit to the tested mixture models for datasets of this measurement type.

Based on proposals by Sylvester (2007), a MLE goodness-of-fit procedure based on the KS test (Clauset et al., 2009) was also implemented for assessing the fit of the datasets to a bimodal lognormal distribution. The test was applied only in sections where EM and BIC mixture analysis recognised bimodal lognormal components for event bed thickness datasets. Results indicate that in most cases the empirical datasets pass a simple KS test at a 5% significance level ($p\text{-value} > 0.05$), but they cannot pass a strict bootstrap KS test (Clauset et al., 2009) at a 10% significance level (Table 11). Only data from the medial Upper S1 section seem to pass the bootstrap KS test for a bimodal lognormal distribution of event thicknesses.

Table 11: Results of the Kolmogorov-Smirnov (KS) goodness-of-fit test based on Clauset et al. (2009) for the bimodal lognormal distribution for turbidite event thicknesses from studied sections.

Section	Mixing Proportions (%)	Mean 1	Mean 2	Standard Deviation 1	Standard Deviation 2	Simple KS Test p-value ($\alpha=0.05$)	KS Test Bootstrap p-value ($\alpha=0.10$)
		(Log cm)	(Log cm)	(Log cm)	(Log cm)		
S2 Lower	78 - 22	2.51	5.39	0.87	0.70	0.52	0.01
S1 Upper	72 - 28	2.53	4.90	0.83	0.88	0.92	0.25
S5	75 - 25	2.15	3.91	0.61	1.19	0.37	0.00
S7	68 - 32	2.12	3.90	0.64	1.15	0.00	0.00

Facies Clustering Results

Hurst classic K and periodogram H estimation

The values of Hurst K and periodogram H and also the number of standard deviations of K and H, of the original series, from the mean K and H of 300 randomly shuffled series were estimated. This was carried out for the coarse division bed thickness and thickness percentage of the coarse divisions (the ratio of coarse divisions to overlying mudstone) in percent for each section (Tables 12-15).

Coarse division thickness

All studied sections exhibit Hurst phenomenon (K or $H > 0.5$) but the observed facies clustering seems to be statistically significant in three out of six studied outcrops for Hurst K and in six out of seven studied outcrops for the Hurst H case. Hurst K statistic was not estimated for the Braux onlap section because that outcrop dataset contains less than 100 measured beds. Data from S2 Lower and S1 Upper sections failed to pass the one-tailed test for randomness exhibiting higher proportion of shuffled sequences with larger or equal K than the original sequence at a significance level $\alpha = 0.1$ (Table 12). The latter observation indicates that in these cases the observed Hurst phenomenon is a product of random processes and not statistically significant. Interpretation of depositional environment based on Hurst K statistic using the criteria of Chen and Hiscott (1999) and Felletti and Bersezio (2010b) (for onlap terminations) indicates a basin floor, sheet sand environment for all the other studied sections (Fig. 6). Similar interpretation of the depositional environment based on Hurst H using the above criteria indicates a basin floor/sheet sand environment for Peira Cava S2 Lower and S5 sections, a lobe-interlobe environment for S2 Upper, S7 and S1 Upper sections and an onlap termination signature for Le Ruch and Braux sections (Fig. 6).

Coarse division thickness percentage

All studied sections exhibit Hurst phenomenon (K or $H > 0.5$) except from Peira Cava S2 Lower section which exhibits a Hurst H lower than 0.5. The observed facies clustering seems to be statistically significant in all of the rest studied outcrops for Hurst K and in five out of seven studied outcrops for the Hurst H case. Data from Peira Cava S1 Upper section failed to pass the one-tailed test for randomness exhibiting higher proportion of shuffled sequences with larger or equal H than the original sequence at a significance level $\alpha = 0.1$. Hurst K statistic for the Braux onlap section was not estimated due to the smaller dataset. Interpretation of depositional environment based on Hurst K statistic using the criteria of Chen and Hiscott (1999) and Felletti and Bersezio (2010b) (for onlap terminations) indicates a basin floor/sheet sand environment for Peira Cava S1 Upper, S2 Lower, S2 Upper S5 and Le Ruch sections and a lobe-interlobe environment for S7 section (Fig. 5). Similar interpretation of depositional environment based on Hurst H using the above criteria indicates a basin floor/sheet sand environment for Peira Cava S5, S2 Upper and Le Ruch sections, a lobe-interlobe environment for Peira Cava S7 section and an onlap termination signature for Braux onlap section (Fig. 5).

Table 12: Hurst K values (classic estimation), deviation of mean K and one-tailed test for randomness for sandstone thickness of studied sections.

Section	Hurst K (Sand Thickness)	Deviation of mean K (300 shuffled sequences)	One-tailed test for randomness ($\alpha=0.05$)
S2 Lower	0.63	0.53	0.28
S1 Upper	0.65	0.91	0.17
S2 Upper	0.69	2.88	0.00
S5	0.64	1.36	0.09
S7	0.67	2.66	0.00
Le Ruch	0.74	2.27	0.00
Braux	-	-	-

Table 13: Hurst K values (classic estimation), deviation of mean K and one-tailed test for randomness for sandstone to mudstone thickness ratio percentage of studied sections.

Section	Hurst K (Sand/Mud Thickness %)	Deviation of mean K (300 shuffled sequences)	One-tailed test for randomness ($\alpha=0.05$)
S2 Lower	0.70	1.49	0.08
S1 Upper	0.70	1.60	0.05
S2 Upper	0.68	2.69	0.00
S5	0.65	1.73	0.03
S7	0.74	4.67	0.00
Le Ruch	0.69	1.31	0.08
Braux	-	-	-

Table 14: Hurst H values (GPH-periodogram estimation), deviation of mean H and one-tailed test for randomness for sandstone thickness of studied sections.

Section	Hurst H (GPH Estimation- Sand Thickness)	Deviation of mean H (300 shuffled sequences)	One-tailed test for randomness ($\alpha=0.05$)
S2 Lower	0.75	2.96	0.00
S1 Upper	0.89	4.53	0.00
S2 Upper	0.64	4.08	0.00
S5	0.56	1.57	0.06
S7	0.62	4.11	0.00
Le Ruch	0.90	3.43	0.00
Braux	0.82	2.23	0.01

Table 15: Hurst H values (GPH-periodogram estimation), deviation of mean H and one-tailed test for randomness for sandstone to mudstone thickness ratio percentage of studied sections.

Section	Hurst H (GPH Estimation- Sand/Mud Thickness %)	Deviation of mean H (300 shuffled sequences)	One-tailed test for randomness ($\alpha=0.05$)
S2 Lower	0.48	-	-
S1 Upper	0.59	0.95	0.18
S2 Upper	0.58	2.11	0.01
S5	0.60	2.59	0.00
S7	0.63	4.93	0.00
Le Ruch	0.76	2.10	0.02
Braux	0.85	2.48	0.01

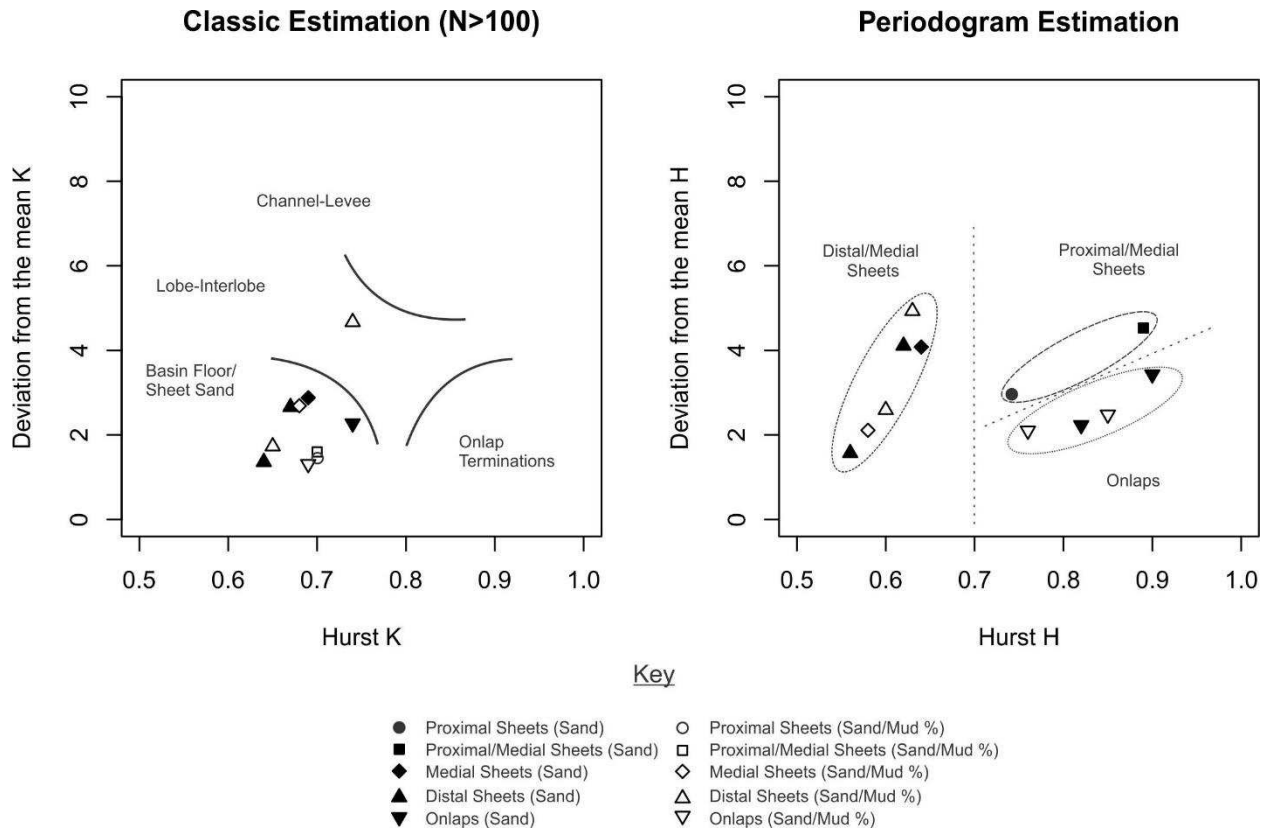


Figure 5: Plots of (statistically significant at the $\alpha=10\%$ significance level) estimated Hurst K and periodogram H values against deviation from mean K and H of 300 shuffled sequences (using Monte Carlo simulation) for coarse division thicknesses and thickness percentages of studied outcrops. Classic Hurst K estimation is based on Hurst (1951) and Chen and Hiscott (1999) for logs with $N>100$. Sub-environment discrimination fields proposed by Chen and Hiscott (1999) and Felletti and Bersezio (2010b) can be also observed. Hurst H periodogram estimation is based on Geweke and Porter-Hudak (1983). Discrimination of onlap sediments from medial/distal sheet deposits can be observed in the plot of the periodogram estimation case in which a possible additional discrimination of proximal/medial sheet deposits may be also possible.

Discussion

Statistical distribution fitting

Generally the theoretical distribution models tested seem to have varying fits depending upon the model tested. Power law and exponential distributions were observed to fit better to coarse division thicknesses, but seem to hold only above a thickness threshold, which varies depending on the

distribution tested and usually represents less than 30% of the whole bed population (Tables 3, 4, 7, 8). Therefore, it can be said that the studied confined mini-basin bed thickness data are characterized by power law and especially exponential thick-bedded tails.

Lognormal theoretical models appear to fit better to event bed thickness populations compared with lithological (coarse division) thickness populations but again they seem to hold only above a thickness threshold, which also usually represents less than 30% of the whole bed population, with the exception of the Braux onlap section.

By contrast, results from previous statistical analysis indicate that most of the tested bed thickness populations can be fitted by a multimodal lognormal model both for the coarse division and event bed thicknesses, which characterize the majority of sampled thickness populations well. Observed lognormal components vary from one to three, with most datasets characterized by a bimodal lognormal model. Furthermore, the fitted composite lognormal models better characterize event thicknesses compared to coarse division thicknesses, exhibiting higher BIC values (Tables 9, &10).

However, the fitted bimodal lognormal mixture models fail to pass a strict bootstrap KS goodness-of-fit test for event bed thicknesses in most cases (Table 11). This could be the result of the large number of measurements (see also Sylvester, 2007) or the result of partial recording of hemipelagic deposits along with turbidite mudstone thicknesses due to discrimination difficulties during logging.

In addition to goodness-of-fit tests, cumulative distribution function (CDF) and quantile-quantile (Q-Q) plots are also useful in choosing the distribution model that provides a better fit. On this kind of plots, the quantiles of the data are plotted against the quantiles of the model distribution and the degree of deviation of the two plotting lines can be assessed graphically. The CDF and Q-Q plots for the fit of a lognormal mixture model to the studied datasets (Fig. 5) indicate that this kind of mixture model

provides a good fit for the whole bed thickness range, and the best fit among the statistical models tested in most of the studied cases.

Origins of mixture components

The observation that sedimentation (event) thicknesses show a better fit to a lognormal mixture model compared to lithological (coarse division) thicknesses probably indicates a sedimentological background process which is related to the observed mixtures.

Authors of previous studies proposed that the frequency of turbidite bed thickness is bimodal, with modes representing thick- and thin-bedded turbidites (Ricci Lucchi and Valmori, 1980). Thicker beds commonly comprise what is interpreted as a thick high-density turbidity current deposit (Lowe S₃ and Bouma T_a divisions) that is often relatively coarse, and a thinner overlying low-density turbidity current deposit interval that is finer-grained (Bouma T_b, T_c and T_d divisions). Thinner beds commonly comprise only low-density turbidity current deposits with finer grain sizes (Bouma, 1962; Talling et al., 2007; 2012). The origins of the bimodality were previously attributed to factors such as sampling bias in favour of thicker beds, deposition in channels and levees, flow reflection or existence of multiple sediment sources (Pirmez et al., 1997).

Based on the observed thickness bimodality in the Marnoso-Arenacea Formation (NE Italy), Talling (2001) proposed a lognormal mixture model for turbidite bed thicknesses, which is probably reflecting the differences in sedimentation rates between more dilute and denser suspensions (low-density and high-density turbidity currents of Lowe, 1982). These two modes of deposition can occur from the same flow. Additional studies in Japan (Kiyosumi Formation) and the Marnoso-Arenacea Formation suggest that the bimodality in bed thicknesses can be also related to a characteristic "top hat" or "core and drape" bed geometry, with beds that are relatively thick in proximal settings rapidly thinning towards more distal areas (Tokuhashi, 1979; Talling et al., 2007; 2012 and references therein).

Conversely, the bimodality of turbidite bed thicknesses could reflect the difference between competence-driven and capacity-driven sedimentation (Hiscott, 1994; Kneller and McCaffrey, 2003; Sylvester, 2007).

Based on numerical analysis, results of the present study confirm the existence of this thickness bimodality for the majority of studied turbidite outcrops, and also even showed the existence of three bed thickness modes in some cases. In order to investigate whether the observed multi-modality reflects the occurrence of dense and/or dilute flow components, a simple comparison test was utilized especially for event bed thickness data from the Peira Cava basin (Table 16): In each bed thickness dataset, the percentage of beds characterized by particular types of Lowe or Bouma sequences was recorded and compared with the percentages of mixing probabilities extracted by EM/BIC analysis (Table 9)

Table 16: Percentages of observed types of Lowe /Bouma sequences of the studied datasets. Their cumulative percentage seems to have similarities with the one characterizing the mixing probability of EM/BIC extracted thickness components.

Section	Type of Lowe/Bouma Sequence	Percentage (%)	Related EM/BIC Analysis Components (Table...)
S2 Lower (Proximal)	S_1-S_3/T_{abcde}	15	Thick-bedded (24.5%)
	S_1-S_3/T_{abce}	2	
	S_1-S_3/T_{abe}	3	
	S_1-S_3/T_a	4.5	Thin-bedded (75.5%)
	T_{abcde}	19	
	T_{bcde}	6.5	
	T_{cde}	8	
	T_{ce}	40.5	
	T_{de}	1.5	
S1 Upper (Medial)	S_1-S_3/T_{abcde}	0.5	Thick-bedded (30.5%)
	S_1-S_3/T_{abce}	3	
	S_1-S_3/T_{abe}	15	
	S_1-S_3/T_a	12	Thin-bedded (69.5%)
	T_{acde}	21	
	T_{bcde}	8	

	T_{cde}	2	
	T_{ce}	38	
	T_{de}	0.5	
S2 Upper (Medial)	S_1-S_3/T_{abcde}	6	Thick-bedded (20.5%)
	S_1-S_3/T_{abce}	0.5	
	S_1-S_3/T_{ace}	8	
	S_1-S_3/T_a	1	
	T_{abcde}	5	
	T_{bcde}	9.5	Thin-bedded (79.5%)
	T_{cde}	11	
	T_{ce}	58.5	
	T_{de}	0.5	
S5 (Distal)	S_1-S_3/T_{abcde}	5	Thick-bedded (25%)
	S_1-S_3/T_{abce}	2	
	S_1-S_3/T_{acde}	16	
	S_1-S_3/T_a	2	
	T_{abcde}	6	Thin-bedded (75%)
	T_{bcde}	6	
		T_{cde}	9
	T_{ce}	53	
	T_{de}	1	
S7 (Distal)	S_1-S_3/T_{abcde}	6	Thick-bedded (35.5%)
	S_1-S_3/T_{abce}	4	
	S_1-S_3/T_{ace}	9	
	S_1-S_3/T_a	2	
	T_{abcde}	7	
	T_{bcde}	4.5	
		T_{cde}	3
	T_{ce}	59.5	Thin-bedded (64.5%)
	T_{de}	5	

This comparison showed a similarity between percentages of the extracted mixing components and those of beds characterized by different sedimentary sequences. In the studied sections, the extracted thick-bedded component seem to be representing beds characterized by basalLow S_1-S_3 /Bouma T_a sequences deposited by high-density flows. On the contrary, beds related with upper parts of Bouma divisions at their bases, seem to express the thin-bedded component of the thickness

datasets. For S2 Upper section, where a three parameter lognormal model was detected, it seems that the two larger thin-bedded modes are related with beds characterized by upper Bouma divisions, and the complex model could be related to EM/BIC overfitting of the low-density bed population. However, again there is a close resemblance of the thicker-bedded lognormal component extracted, with percentages of beds with basal Lowe S_1 - S_3 / T_a beds (Table 16).

Summarizing, results shown in Table 16 strongly suggest that the lognormal components detected by the EM/BIC mixture model analysis seem to have a sedimentological origin and are mainly related to beds deposited by dense and more dilute flows respectively, confirming previous observations (Talling, 2001; Sylvester, 2007; Pantopoulos et al., 2013).

Discrimination of architectural elements

Bed thickness distribution

Previous studies questioned the possibility of using turbidite bed thickness distributions to give general indications of the depositional characteristics of turbidite systems when used alone, due to the degree of complexity that can be observed in turbidite systems worldwide (Sylvester, 2007). However they pointed out the potential usefulness of some statistical parameters in differentiating depositional settings (Malinverno, 1997; Carlson and Grotzinger, 2001; Mattern, 2002; Sinclair and Cowie, 2003; Clark and Steel, 2006; Sylvester, 2007), even when working with data of limited lateral extent, such as wells and smaller outcrops, especially when combined with other types of data e.g. seismic, wireline well-log, etc.

Based on previous proposals and observations from data analysis of the present study, a discrimination of the different architectural elements sampled was attempted based on parameters of the fitted statistical distribution models.

Statistical distribution fitting results indicate that a discrimination of depositional environments based on deviations from a power law bed thickness distribution as proposed by previous studies (Carlson and Grotzinger, 2001; Sinclair and Cowie, 2003) is not possible for the studied turbidites: bed thickness data from proximal as well as distal confined sheet and heterolithic deposits both exhibited poor fits to a power law (Tables 3, 4). Even in cases of a good fit, the power law seems to hold only for a portion of thicker beds (power law tail). However, based on the occurrence of power law tails, some discrimination can be made between the sampled outcrop datasets. Onlap sections seem to exhibit power law tails for the coarse division or event thickness in both studied sections.

Power law distributions for coarse division thickness populations were also observed by Marini et al. (2016) in turbidite deposits from Tertiary confined basins of the central-northern Apennines in Italy and were attributed as a signature of flow confinement, characterizing only the thicker basin-wide ponded beds. In the present study, the thick-bedded power law tail which seems to characterize the coarse division thicknesses of outcrops S1 Upper and S7 seems to hold for beds thicker than 170 cm and 240 cm respectively (Table 3), including basin-wide marker megabeds, agreeing with the proposals of Marini et al. (2016). However, Pantopoulos et al. (2013) also observed these power law tails in turbidite sediments deposited in various depositional settings of the Hellenide fold and thrust belt in Greece and further investigation is needed on the subject.

Also, it seems that discrimination between different architectural elements based on the exponential distribution is not feasible. The majority of sampled outcrops show a good fit to an

exponential distribution above a thickness threshold (exponential tail) both for the coarse division and event thicknesses regardless of the architectural element sampled (Tables 7, 8).

Instead, a better fit to a multimodal lognormal distribution model is observed for all the studied datasets. In most cases this multimodal mixture model seems to consist of two lognormal modes. Based on the latter statistical theoretical model that gave the best fitting results, an attempt was made to distinguish the studied architectural elements. The attempt was focused on detecting differences between the number of detected components and their variabilities as also proposed by Sylvester (2007).

Figure 6 and Table 17 show the difference of observed lognormal mixture models of event thicknesses for sampled stratigraphic intervals of the Peira Cava confined mini-basin. Proximal and proximal to medial sheets and heterolithic deposits of the Lower S2 and Upper S1 sections seem to be characterized by a bimodal lognormal distribution with the two components having equal variances (2E). Medial sheets and heterolithics of the Upper S2 section are characterized by a more complex lognormal mixture of three components with different variances (3V). Distal sheet and heterolithic deposits of sections S5 and S7 are both characterized by similar bimodal lognormal distributions, with the two components having unequal variances (2V). Particularly in distal sheet and heterolithic deposits, both observed bimodal lognormal distributions are characterized by a thin-bedded component with smaller variance compared to its thick-bedded counterpart. Also, both detected components seem to be characterized by similar mean and standard deviation values in both studied (S5, S7) distal sections.

Table 17: Difference of observed lognormal mixture model parameters of the coarse division and event thicknesses for sampled stratigraphic intervals of the Peira Cava mini-basin. Detected lognormal components number and equality (E) or non-equality (V) of their variances is indicated. Existence or not of power law tails can be also observed.

Architectural Element	Detected Lognormal Components (Coarse Divisions)	Thin-Thick Beds Mixing Probabilities (Coarse Divisions)	Thick Bed Power Law Tails (Coarse Divisions)	Detected Lognormal Components (Events)
Basin Margin Onlaps	1/2E	85-15	√	1/2E
Proximal Sheets/Heterolithics	3E	50-50	x	2E
Medial Sheets/Heterolithics	2E/2V	65-35/75-25	√/x	2E/3V
Distal Sheets/Heterolithics	2E/3V	85-15/90-10	√/x	2V

Differences between the sampled architectural elements can be also observed by the characteristics of components detected for coarse division thicknesses both for component variances and also for mixing probabilities of the observed components, with the more distal sections showing lower mixing probabilities of the thick-bedded component (Table 17).

Based on observations made in the previous section that link the observed lognormal modes to beds deposited by different sedimentation mechanisms, it can be deduced that the observed lognormal mixture patterns probably reflect the higher importance of the thick-bedded (dense flow- or capacity - derived) component in the more proximal sections, the effects of which are less in the distal sections. It is also possible that the differences in the lognormal mixture patterns seen across the Peira Cava basin, reflect the asymmetrical cross current facies distribution and the larger effect of reflection processes in the more distal parts of the basin characterized by large abundances of contained-reflected beds with convolute laminations (Bouma T_c divisions, see also Cunha et al., 2017).

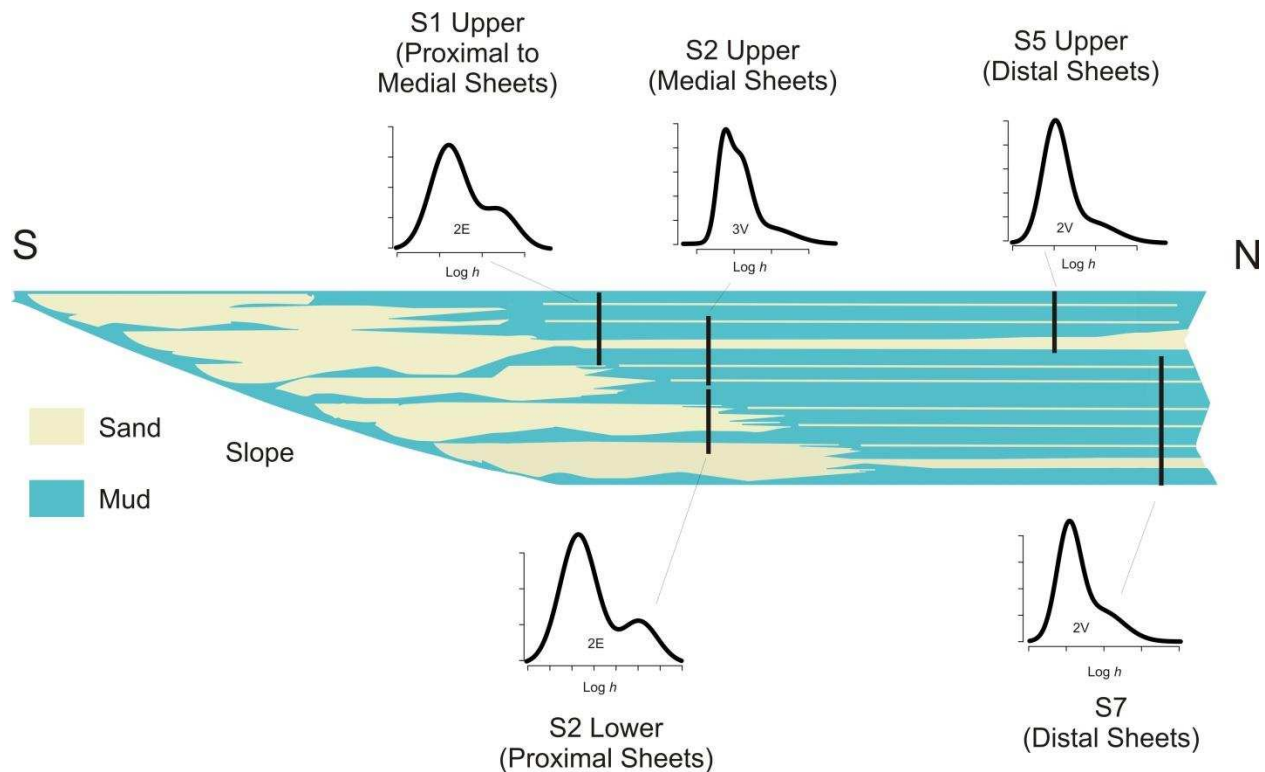


Figure 6: Diagram illustrating lognormal mixture distribution patterns of event bed thicknesses that represent different architectural elements sampled in Peira Cava confined mini-basin (SE France). Number of lognormal components detected and difference (V) or equality (E) of their variances is also illustrated. Diagram not to scale, modified from Amy et al. (2007).

Facies clustering

Results of facies clustering analysis both for the coarse division thickness and thickness percentage from all the studied outcrops allow us to extract useful conclusions regarding the usage of the Hurst statistic as a tool for discriminating architectural elements in ancient confined deep-water deposits. Observations can also be made regarding the performance of each Hurst exponent estimation technique (classic K or periodogram H) in the successful discrimination of sampled architectural elements.

Hurst K results (Fig. 6) broadly agree with observations made of bed continuity in the Peira Cava basin, indicating large lateral extent of beds. Sheets are the most common element of the Peira Cava system, with previous correlations (Amy, 2000) demonstrating that most beds of the Peira Cava basin do

not show significant thickness changes over kilometers and that many beds display facies indicative of lobe and channel-lobe transition environment, especially at the southern more proximal part of the basin (Tinterri et al., 2016; Cunha et al., 2017). Although most of the system is composed of sheets, the geometry of these may be complex because of variations in the stacking pattern (Amy, 2000). On the other hand, Hurst K classification results do not compare well with sedimentological interpretations for the Le Ruch onlap section.

Classification based on periodogram estimation of Hurst H (Fig. 5) works better for distinguishing onlap deposits based on previous proposed classifications (Felletti, 2004; Felletti and Bersezio, 2010b) and also for recognizing the more distal to medial components of the Peira Cava basin which exhibit lower degrees of clustering (Fig. 6). Proximal to medial architectural elements can be also distinguished, showing larger degrees of clustering but higher deviations of the mean H value.

Implications for petroleum exploration in deep-water confined mini-basins

Determination of the depositional elements of a basin's fill, is of great interest in petroleum geology, especially when considering development plans for hydrocarbon fields. Usually, detailed sedimentological analysis based on extensive outcrop exposures is needed for potential identification of depositional elements of deep-marine systems (e.g. Reading and Richards, 1994; Galloway, 1998; Morris and Normark, 2000; Browne et al., 2005; Posamentier and Walker, 2006). In cases of subsurface studies when outcrop data are absent, depositional element identification is mainly based on well log data (Richards and Bowman, 1998; Weimer and Slatt, 2007), often calibrated upon outcrop analogues, sometimes of doubtful applicability.

In the case of confined mini-basins, depositional components often include ponded, amalgamated and heterolithic layered sheets in proximal and more distal basin areas, as well as basin margin facies onlapping the substrate (e.g. McCaffrey and Kneller, 2001; Amy et al., 2007). Consequently, differentiation of these ponded depositional elements is of great importance in hydrocarbon exploration since the reservoir properties of these elements differ, with great impact on reservoir facies distribution and performance. The present work constitutes an architectural elements differentiation approach which proposes a number of statistical criteria based on frequency distribution and facies clustering analysis (Table 17). The latter in combination with sedimentological criteria and the use of other types of data (e.g. palynofacies, see also McArthur et al., 2016) could be extracted from subsurface datasets in order to assist the identification of architectural elements in the subsurface, and to evaluate their reservoir potential.

Conclusions

Based on the above bed thickness statistical analysis of well-documented architectural elements from confined mini-basins of SE France the following observations can be drawn:

- Turbidite bed thickness data seems to be best characterized by a mixture of lognormal distributions for the whole bed thickness range. The observed lognormal mixtures are a better fit for sedimentation rather than lithological thickness populations, indicating a sedimentological background mechanism which possibly reflects the difference between deposition from both low- and high-density turbidity currents or the difference between competence- and capacity-driven sedimentation.

- Power law and exponential distributions were observed to hold only for the thick-bedded tails of some of the studied datasets and they fit better to lithological rather than sedimentation thickness populations. Power law tails were particularly observed to hold for the thick-bedded thickness population of the studied basin margin onlap deposits.
- Discrimination of architectural elements in the studied successions is feasible based on the characteristics of the observed lognormal mixtures such as number and variability of the detected components. The latter parameters can be objectively extracted through a robust statistical procedure. The studied successions also exhibit non-random clustering of bed thickness both for classic Hurst K and periodogram Hurst H values. The estimation of the degree of clustering based on the periodogram method has the potential to discriminate architectural elements in confined basin settings and in some cases performs better than previously proposed estimation methods.
- Based on parameters extracted from the above analysis a selection of criteria is proposed, which in combination with other types of data can aid the discrimination of architectural elements in less certain confined mini-basin settings, e.g. in the subsurface.

Acknowledgements

This study was part of the DMS Tools Project, executed at Universidade Federal do Rio Grande do Sul (UFRGS), to which the first author is grateful for a post-doctorate scholarship grant. We also thank Shell and former BG Brasil for financial support and permission to publish results. The Agência Nacional do Petróleo (ANP) also supported this project under the Brazilian Petroleum Law for research commitment clauses. Sven Egenhoff is thanked for editorial handling. Constructive comments and criticisms by Carl Drummond and an anonymous reviewer improved an initial version of this manuscript.

References

Amy, L.A. 2000. Architectural analysis of a sand-rich confined turbidite basin: the Grès de Peïra Cava, SE France. Unpublished PhD thesis, University of Leeds, UK.

Amy, L.A., McCaffrey, W.D. & Kneller, B.C. 2000. Evaluating the links between turbidite characteristics and gross system architecture: upscaling insights from the turbidite sheet-system of Peïra Cava, SE France. In: Weimer, P., Slatt, R.M. & Coleman, J. et al. (eds) Deep Water Reservoirs of the World. Gulf Coast Section SEPM Foundation 20th Annual Research Conference. SEPM, Houston, TX (CD-ROM), 1-15.

Amy, L.A., McCaffrey, W.D. & Kneller, B.C. 2004. The influence of a lateral basin-slope on the depositional patterns of natural and experimental turbidity currents. In: Joseph, P. & Lomas, S.A. (eds) Deep-Water Sedimentation in the Alpine Foreland Basin of SE France: New Perspectives on the Grès d'Annot and Related Systems. Geological Society, London, Special Publications, 221, 311-330.

Amy, L.A., Kneller, B.C. & McCaffrey, W.D. 2007. Facies architecture of the Grès de Peïra Cava, SE France: Landward stacking patterns in ponded turbiditic basins. Journal of the Geological Society of London, 164, 143-162.

Apps, G. 1987. Evolution of the Gres d'Annot basin, SW Alps. Unpublished PhD Thesis, University of Liverpool, UK.

Apps, G., Peel, F. & Elliott, T. 2004. The structural setting and palaeogeographical evolution of the Grès d'Annot Basin. In: Joseph, P. & Lomas, S. A. (eds) 2004. Deep-Water Sedimentation in the Alpine Basin of SE France: New perspectives on the Grès d'Annot and related systems. Geological Society, London, Special Publications, 221, 65-96.

Bouma, A. H. 1962. Sedimentology of some flysch deposits: a graphic approach to facies interpretation. Elsevier Publication, Amsterdam, 6, 168p.

Browne, G.H., King, P.R. Higgs, K. E. & Slatt, R.M. 2005. Grain-size characteristics for distinguishing basin floor fan and slope fan depositional settings: outcrop and subsurface examples from the late Miocene Mount Messenger Formation, New Zealand. *New Zealand Journal of Geology and Geophysics*, 48, 213-227.

Carlson, J. & Grotzinger, J.P. 2001. Submarine fan environment inferred from turbidite thickness distributions. *Sedimentology*, 48, 1331-1351.

Chen, C. & Hiscott, R.N. 1999. Statistical analysis of facies clustering in submarine-fan turbidite successions. *Journal of Sedimentary Research*, 69, 505-517.

Clark, B.E., & Steel, R.J. 2006. Eocene turbidite-population statistics from shelf edge to basin floor, Spitsbergen, Svalbard. *Journal of Sedimentary Research*, 76, 903-918.

Clauset, A., Shalizi, C.R. and Newman, M.E.J. 2009. Power-law distributions in empirical data. *SIAM Review*, 51, 661-703.

Cunha, R.S., Tinterri, R. and Muzzi Magalhaes, P. 2017. Annot Sandstone in the Peira Cava basin: An example of an asymmetric facies distribution in a confined turbidite system (SE France). *Marine and Petroleum Geology* 87, 60-79.

Drinkwater, N.J. & Pickering, K.T. 2001. Architectural elements in a high-continuity sandprone turbidite system, Late Precambrian Kongsfjord Formation, Northern Norway: application to hydrocarbon reservoir characterization. *AAPG Bulletin*, 85, 1731-1757.

du Fornel, E., Joseph, P., Desaubliaux, G., Eschard, R., Guillocheau, F., Lerat, O., Muller, C., Ravenne, C., Sztrakos, K., 2004. The southern Gres d'Annot outcrops (French Alps): an attempt at regional correlation. In: Joseph, P., Lomas, S.A. (Eds.), Deep Water Sedimentation in the Alpine Basin of SE France. New Perspectives on the Grés d'Annot and Related Systems. Special Publications, Geological Society, London, pp. 137-160.

Elliott, T., Apps, G., Davies, H., Evans, M., Ghibaudo, G. & Graham, R.H. 1985. Field excursion B: a structural and sedimentological traverse through the Tertiary foreland basin of the external Alps of South-east France. In: Allen, P.A. & Homewood, P. (eds) Field Excursion Guide Book, International Association of Sedimentologists, Meeting on Foreland Basins. 39-73.

Felletti, F. 2004. Spatial variability of Hurst statistics in the Castagnola Formation, Tertiary Piedmont Basin, NW Italy: discrimination of sub-environments in a confined turbidite system. In: Lomas, S.A., Joseph, P. (Eds.), Confined Turbidite Systems. Geological Society of London, Special Publications, 222, 285-305.

Felletti, F. & Bersezio, R. 2010. Validation of Hurst statistics: a predictive tool to discriminate turbiditic sub-environments in a confined basin. *Petroleum Geoscience*, 16, 401-412.

Flint, S. & Bryant, I.D. 1993. The geological modelling of hydrocarbon reservoirs and outcrop analogues. *International Association of Sedimentologists Special Publication*, 15, 1-269.

Fraley, C. & Raftery, A. 2002. Model-based clustering, discriminant analysis and density estimation. *Journal of the American Statistical Association* 97, 611-631

Fraley, C., Raftery, A. E., Murphy, T. B. and Scrucca, L. 2012. mclust Version 4 for R: Normal Mixture Modeling for Model-Based Clustering, Classification, and Density Estimation. Technical Report No. 597, Department of Statistics, University of Washington, 57p.

Galloway, W. E. 1998. Siliciclastic Slope and Base-of-Slope Depositional Systems: Component Facies, Stratigraphic Architecture, and Classification. *AAPG Bulletin*, 82, 569-595.

Geweke, J. and Porter-Hudak, S. 1983. The estimation and application of long-memory time series models. *Journal of Time Series Analysis*, 4, 221-237.

Ghibaudo, G. 1995. Sandbody geometries in an onlapping turbiditic basin fill: Montagne de Chalufy, Alpes des Hautes Provence, SE France. *Atlas of Deep Water Environments*, Chapman and Hall. Ed.s Pickering, K.T., Hiscott, R.N., Kenyon, N.H., Ricci Luchi, F and Smith, R.D.A., 242-243.

Gillespie, C. 2015. Fitting Heavy Tailed Distributions: The powerLaw Package. *Journal of Statistical Software*, 64, 16p.

Hilton, V.C. 1994. Architecture of deep-marine confined sandstone bodies, Eocene-Oligocene Grès d'Annot Formation SE France. Unpublished PhD thesis, University of Leicester.

Hilton, V.C. and Pickering, K.T. 1995. The Montagne de Chalufy turbidite onlap, Eocene-Oligocene turbidite sheet system, Hautes Provence, SE France. *Atlas of Deep Water Environments*, Chapman and Hall. Ed.s Pickering, K.T., Hiscott, R.N., Kenyon, N.H., Ricci Luchi, F and Smith, R.D.A., 236-241.

Hiscott, R.N. 1994. Loss of capacity, not competence, as the fundamental process governing deposition from turbidity currents. *Journal of Sedimentary Research*, A64, 209-214.

Hurst, H.E. 1951. Long term storage capacity of reservoirs. *Transactions of the American Society of Civil Engineers*, 116, 770-808.

Joseph, P. & Lomas, S.A. 2004. Deep-water sedimentation in the Alpine Foreland Basin of SE France: new perspectives on the Grès d'Annot and related turbidite systems: an introduction. In: Joseph, P. & Lomas,

S.A. (eds) Deep-Water Sedimentation in the Alpine Foreland Basin of SE France: New Perspectives on the Gre` s d'Annot and Related Systems. Geological Society, London, Special Publications 221, 1-17.

Kneller, B. & McCaffrey, W., 1999. Depositional effects of flow nonuniformity and stratification within turbidity currents approaching a bounding slope: deflection, reflection, and facies variation. *Journal of Sedimentary Research*, 69, 980-991.

Kneller, B.C., McCaffrey, W.D., 2003. The interpretation of vertical sequences in turbidite beds: the influence of longitudinal flow structure. *Journal of Sedimentary Research* 73, 706-713.

Kötelešová, S. 2012. Facies clustering in deep-water successions of the Magura zone of the Outer Western Carpathians: implications for interpretation of submarine-fan environments. *Facies*, 58, 217-227.

Lee, S.E., Amy, L.A. and Talling, P.J. 2004. The character and origin of thick base-of-slope sandstone units of the Peira Cava outlier, SE France. In: Joseph, P. & Lomas, S.A. (Eds.), *Deep-Water Sedimentation in the Alpine Foreland Basin of SE France: New Perspectives on the Gre` s d'Annot and Related Systems*. Geological Society, London, Special Publications, 221, 331-347.

Lowe, D.R. 1982. Sediment gravity flows. II. Depositional models with special reference to the deposits of high-density turbidity currents. *Journal of Sedimentary Petrology*, 52, 279-297.

Malinverno, A. 1997. On the power law size distribution of turbidite beds. *Basin Research*, 9, 263-274.

Marini, M., Felletti, F., Milli, S. and Patacci, M. 2016. The thick-bedded tail of turbidite thickness distribution as a proxy for flow confinement: Examples from tertiary basins of central and northern Apennines (Italy). *Sedimentary Geology*, 341, 96-118.

Mattern, F. 2002. Amalgamation surfaces, bed thicknesses, and dish structures in sand-rich submarine fans: Numeric differences in channelized and unchannelized deposits and their diagnostic value. *Sedimentary Geology* 150, 203-228.

McArthur, A.D., Kneller, B.C., Wakefield, M.I., Souza, P.A. and Kuchle, J. 2016. Palynofacies classification of the depositional elements of confined turbidite systems: Examples from the Gres d'Annot, SE France. *Marine and Petroleum Geology* 77, 1254-1273.

McCaffrey, W.D. & Kneller, B.C. 2001. Process controls on the development of stratigraphic trap potential on the margins of confined turbidite systems, and aids to reservoir evaluation. *AAPG Bulletin*, 85, 971–988.

Morris, W.R. & Normark, W.R. 2000. Sedimentologic and geometric criteria for comparing modern and ancient sandy turbidite elements. In: Weimer, P. Slatt, R.M. Coleman, J.L. Rosen N., Nelson C.H., Bouma A.H., Styzen, M. & Lawrence, D.T. (Eds.), *Global Deep-Water Reservoirs: Gulf Coast Section-SEPM Foundation 20th Annual Bob F. Perkins Research Conference*, 606-623.

Mukhopadhyay, B., Chakraborty, P.P., Paul, S., 2003. Facies clustering in turbidite successions: case study from Andaman Flysch Group, Andaman Islands, India. *Gondwana Research* 6, 918-925.

Palozzi, J., Pantopoulos, G., Maravelis, A.G., Nordsvan, A. and Zelilidis, A. 2018. Sedimentological analysis and bed thickness statistics from a Carboniferous deep-water channel-levee complex: Myall Trough, SE Australia. *Sedimentary Geology* 364, 160-179.

Pantopoulos, G., Vakalas, I., Maravelis, A., and Zelilidis, A. 2013. Statistical analysis of turbidite bed thickness patterns from the Alpine fold and thrust belt of western and southeastern Greece. *Sedimentary Geology* 294, 37-57.

Pirmez, C., Hiscott, R.N. and Kronen, J.D. Jr. 1997. Sandy turbidite successions at the base of channel levee systems of the Amazon Fan revealed by FMS logs and cores: unraveling the facies architecture of large submarine fans. *Proc. ODP Sci. Results*, 155, 7-33.

Posamentier, H.W. & Walker, R.G. 2006. Deep-water turbidites and submarine fans. In: Posamentier, H.W. & Walker R.G. (Eds.), *Facies Models Revisited*. Society for Sedimentary Geology (SEPM), Special Publication 84, 397–520.

Prekopová, M., Janočko, J., 2009. Quantitative approach in environmental interpretations of deep-marine sediments (Dukla Unit, Western Carpathian Flysch Zone). *Geologica Carpathica* 60, 485-494.

Puigdefàbregas, C., Gjelberg, J., and Vaksdal, M. 2004. The Grès d'Annot in the Annot syncline: Outer basin-margin onlap and associated soft-sediment deformation. In: Joseph, P. & Lomas, S.A. (Eds.), *Deep-Water Sedimentation in the Alpine Foreland Basin of SE France: New Perspectives on the Grès d'Annot and Related Systems*. Geological Society, London, Special Publications, 221, 367-388.

R Core Team, 2018. *R: A Language and Environment for Statistical Computing*. R Foundation for Statistical Computing, Vienna, Austria (URL <http://www.R-project.org/>).

Ravenne, C. Vially, R., Riche, Ph. and Tremolieres. 1987. Sedimentation et tectonique dans le bassin marin Eocene superieur - Oligocene des Alpes du Sud. *Revue de l'Institut Francais du petrole* 42, 529-523.

Reading, H.G. & Richards, M. 1994. Turbidite systems in deep-water basin margins classified by grain size and feeder system. *AAPG Bulletin*, 78, 792-822.

Ricci Lucchi, F. & Valmori, E. 1980. Basin-wide turbidites in a Miocene, over-supplied deep-sea plain: a geometrical analysis. *Sedimentology*, 27, 241–270.

Richards, M. & Bowman, M. 1998. Submarine fans and related depositional systems ii: variability in reservoir architecture and wireline log character. *Marine and Petroleum Geology* 15, 821-839.

Sinclair, H.D. 1994. The influence of lateral basinal slopes on turbidite sandstone deposition in the Annot Sandstones of SE France. *Journal of Sedimentary Research* 64, 42-64.

Sinclair, H.D. 1997. Tectonostratigraphic model for underfilled peripheral foreland basins: An Alpine perspective. *Bulletin of the Geological Society of America*, 109, 324-346.

Sinclair, H.D. 2000. Delta-Fed turbidites infilling topographically complex basins: a new depositional model for the Annot sandstones, SE France. *Journal of Sedimentary Research* 70, 504-519.

Sinclair, H.D. & Cowie, P.A. 2003. Basin-floor topography and the scaling of turbidites. *Journal of Geology* 111, 277–299.

Stanbrook, D.A. & Clark, J.D. 2004. The Marnes Brunès Inférieures in the Grand Coyer remnant: Characteristics, structure and relationship to the Grès d'Annot. In: Joseph, P. & Lomas, S.A. (Eds.), *Deep-Water Sedimentation in the Alpine Foreland Basin of SE France: New Perspectives on the Grès d'Annot and Related Systems*. Geological Society, London, Special Publications, 221, 285-300.

Stanley, D.J. & Mutti, E. 1978. Sedimentological evidence for an emerged land mass in the Ligurian Sea during the Palaeocene. *Nature* 218, 32-36.

Stanley, D.J., Palmer, H.D., Dill, R.F., 1978. Coarse sediment transport by mass flow and turbidity current processes and downslope transformations in Annot Sandstone canyon-fan valley systems. *Sediment. Submar. Canyons Fans Trenches* 85-115.

Sylvester, Z. 2007. Turbidite bed thickness distributions: methods and pitfalls of analysis and modelling. *Sedimentology*, 54, 847–870.

Talling, P.J. 2001. On the frequency distribution of turbidite thickness. *Sedimentology*, 48, 1297–1331.

Talling, P.J., Amy, L.A., Wynn, R.B., Blackbourn, G. and Gibson, O. 2007. Evolution of turbidity currents deduced from extensive thin turbidites: Marnoso Arenacea Formation (Miocene), Italian Apennines. *Journal of Sedimentary Research*, 77, 172–196.

Talling, P.J., Masson, D.G., Sumner, E.J. and Malgesini, G., 2012. Subaqueous sediment density flows: depositional processes and deposit types. *Sedimentology* 59, 1937-2003.

Tinterri, R., Muzzi Magalhaes, P., Tagliaferri, A. and Cunha, R.S. 2016. Convolute laminations and load structures in turbidites as indicators of flow reflections and decelerations against bounding slopes. Examples from the Marnoso-arenacea Formation (northern Italy) and Annot Sandstones (south eastern France). *Sedimentary Geology* 344, 382-407.

Tokuhashi, S. 1979. Three Dimensional Analysis of a Large Sandy-flysch Body, Mio-Pliocene Kiyosumi Formation, Boso Peninsula, Japan. *Memoirs of the Faculty of Science, Kyoto University. Series of geology and mineralogy*, 46, 1-60

Weimer P. & Slatt R.M. 2007. Introduction to the petroleum geology of deep-water settings, AAPG Studies in Geology Series, 57, 816 p.

Wuertz, D. 2015. Package 'fArma'. CRAN electronic depository, <https://cran.r-project.org/web/packages/fArma/fArma.pdf>